PITHA 01/02
DESY 01-040
TTP01-11

April 2001

Next-to-leading order QCD corrections to top quark spin correlations at hadron colliders: the reactions $gg \to t\bar{t}(g)$ and $gq(\bar{q}) \to t\bar{t}q(\bar{q})$

W. Bernreuther [a], A. Brandenburg [b,1], Z. G. Si [a,2] and P. Uwer [c]

[a] Institut f. Theoretische Physik, RWTH Aachen, 52056 Aachen, Germany
[b] DESY-Theorie, 22603 Hamburg, Germany
[c] Institut f. Theoretische Teilchenphysik, Universität Karlsruhe, 76128 Karlsruhe, Germany

Abstract:
We have computed the cross section for $t\bar{t}$ production by gluon-gluon fusion at next-to-leading order (NLO) in the QCD coupling, keeping the full dependence on the $t\bar{t}$ spins. Furthermore we have determined to the same order the spin dependent cross sections for the processes $g+q(\bar{q}) \to t\bar{t}+q(\bar{q})$. Together with our previous results [1] for $q+\bar{q} \to t\bar{t}(g)$ these results allow for predictions, at NLO QCD, of the hadronic production of $t\bar{t}$ pairs in a general spin configuration. As an application we have determined the degree of correlation of the t and $\bar{t}$ spins at NLO, using various spin quantisation axes.

PACS number(s): 12.38.Bx, 13.88.+e, 14.65.Ha
Keywords: hadron collider physics, top quarks, spin correlations, QCD corrections

[1] supported by a Heisenberg fellowship of D.F.G.
[2] supported by BMBF contract 05 HT9 PAA 1

In this Letter we report on the calculation of the cross section for $t\bar{t}$ production by gluon-gluon and by (anti)quark-gluon fusion at order α_s^3 in the QCD coupling, keeping the full information on the spin state of the $t\bar{t}$ system. The results presented in this work constitute the last missing ingredient to analyse, at NLO QCD, $t\bar{t}$ production including spin effects at hadron colliders. Together with the corresponding results for $t\bar{t}$ production by quark-antiquark annihilation [1], they extend previous results for the spin-averaged differential $t\bar{t}$ cross section [2, 3, 4, 5].

Analysis of top quark spin phenomena at the upgraded Tevatron and at the Large Hadron Collider (LHC) will play an important role in investigating the interactions of these quarks. (For a recent overview of the perspectives of top quark spin physics at hadron colliders and an extensive list of references, see, e.g., ref. [6].) In the following we first describe the salient features of our computation. Then we determine the correlation of the t and $\bar{t}$ spins at NLO for a number of spin bases.

The theoretical description of $t\bar{t}$ production by proton-proton and proton-antiproton collisions at next-to-leading order in the QCD coupling amounts to considering the following parton reactions: quark-antiquark annihilation

$$q(p_1)+\bar{q}(p_2)\to t(k_t)+\bar{t}(k_{\bar{t}}), \tag{1}$$

$$q(p_1)+\bar{q}(p_2)\to t(k_t)+\bar{t}(k_{\bar{t}})+g(k_3), \tag{2}$$

which is the dominant production mechanism at the Tevatron, gluon-gluon fusion

$$g(p_1)+g(p_2)\to t(k_t)+\bar{t}(k_{\bar{t}}), \tag{3}$$

$$g(p_1)+g(p_2)\to t(k_t)+\bar{t}(k_{\bar{t}})+g(k_3), \tag{4}$$

which dominates at the LHC, and

$$g(p_1)+q(p_2)\to t(k_t)+\bar{t}(k_{\bar{t}})+q(k_3), \tag{5}$$

$$g(p_1)+\bar{q}(p_2)\to t(k_t)+\bar{t}(k_{\bar{t}})+\bar{q}(k_3). \tag{6}$$

In the Standard Model the main top decay modes are $t\to bW\to bq\bar{q}', b\ell\nu_\ell$. Among these final states the charged leptons, or the jets from quarks of weak isospin $-1/2$ originating from the W decay, are the most powerful analysers of the polarisation of the top quark. A complete next-to-leading order QCD analysis thus consists of treating the parton reactions

$$gg, q\bar{q}\to t\bar{t}\to b\bar{b}+4f, \tag{7}$$

$$gg, q\bar{q}\to t\bar{t}\to b\bar{b}+4f+g, \tag{8}$$

$$g+q(\bar{q})\to t\bar{t}\to b\bar{b}+4f+q(\bar{q}), \tag{9}$$

where $f=q,\ell,\nu_\ell$. To leading order in α_s only the reactions (7) contribute. In view of the fact that the total width Γ_t of the top quark is much smaller than its mass, $\Gamma_t/m_t=O(1\%)$, one may analyse the above reactions using the so-called narrow width or leading pole approximation [7, 8]. In the case at hand this approach consists, for a given process, in an expansion of the amplitude around the poles of the unstable t and $\bar{t}$ quarks, which corresponds to an expansion in powers of Γ_t/m_t. Only the leading term of this expansion, i.e., the residue of the double poles is considered here. In this framework the radiative corrections to (7) can be classified into so-called factorisable and non-factorisable corrections. In the case of the gluon radiation processes (8) already the lowest order contributions to the respective squared matrix element $|\mathcal{M}|^2$ decompose into these two groups. We compute the factorisable corrections[3] for which the squared matrix element $\mathcal{M}$ is of the form

$$|\mathcal{M}|^2 \propto \mathrm{Tr}\,[\rho R \bar{\rho}] = \rho_{\alpha'\alpha} R_{\alpha\alpha',\beta\beta'} \bar{\rho}_{\beta'\beta}. \tag{10}$$

Here R denotes the density matrix for the production of on-shell $t\bar{t}$ pairs and $\rho, \bar{\rho}$ are the density matrices describing the decay of polarised t and $\bar{t}$ quarks, respectively, into specific final states. The subscripts in eq. (10) denote the t, $\bar{t}$ spin indices. Because the colours of the final state partons are summed over, $\rho, \bar{\rho}$ are unit matrices in the colour indices of t and $\bar{t}$. This implies that the colour indices of t and $\bar{t}$ are summed over in the computation of R. Note that both the production and decay density matrices are gauge invariant. The one-loop QCD corrections to the density matrices of semileptonic decays of polarised top quarks and of $t \to W + b$ can be obtained from the results of refs. [10] and [11, 12], respectively.

In the calculation of the production density matrices for the reactions (3) – (6) we follow our approach [1] to computing those of reaction (1) and reaction (2). The density matrix for the production process (3) is defined in terms of the transition matrix element as follows:

$$R^{(gg)}_{\alpha\alpha',\beta\beta'} = \frac{1}{N_{gg}} \sum_{\substack{\text{colors}\\ \text{initial spins}}} \langle t_\alpha \bar{t}_\beta | \mathcal{T} | gg \rangle \, \langle gg | \mathcal{T}^\dagger | t_{\alpha'} \bar{t}_{\beta'} \rangle \,, \tag{11}$$

where the factor $N_{gg} = 256$ averages over the spins and colours of the initial pair of gluons. The matrix structure of $R^{(gg)}$ is

$$\begin{aligned} R^{(gg)}_{\alpha\alpha',\beta\beta'} &= A^{(gg)} \delta_{\alpha\alpha'} \delta_{\beta\beta'} + B^{(gg)}_i (\sigma^i)_{\alpha\alpha'} \delta_{\beta\beta'} + \bar{B}^{(gg)}_i \delta_{\alpha\alpha'} (\sigma^i)_{\beta\beta'} \\ &\quad + C^{(gg)}_{ij} (\sigma^i)_{\alpha\alpha'} (\sigma^j)_{\beta\beta'} \,, \end{aligned} \tag{12}$$

where σ^i are the Pauli matrices. Using rotational invariance the 'structure functions' $B^{(gg)}_i, \bar{B}^{(gg)}_i$ and $C^{(gg)}_{ij}$ can be further decomposed. The function $A^{(gg)} = \mathrm{Tr}\,[R^{(gg)}]/4$, determines the $gg \to t\bar{t}$ differential cross section with $t\bar{t}$ spins summed over. Because of parity invariance the vectors $\mathbf{B}^{(gg)}, \bar{\mathbf{B}}^{(gg)}$ can have, within QCD, only a component normal to the scattering plane. This component, which amounts to a normal polarisation of the t and $\bar{t}$ quarks, is induced by the absorptive part of the scattering amplitude which is non-zero to order α_s^3. The normal polarisation is quite small, both for $t\bar{t}$ production at the Tevatron and at the LHC [13, 14]. The functions $C^{(gg)}_{ij}$ encode the correlation between the t and $\bar{t}$ spins. The production density matrices $R^{(gg,g)}$, $R^{(gq,q)}$, and $R^{(g\bar{q},\bar{q})}$ for the reactions

[3] The non-factorisable NLO QCD contributions were studied for gg and $q\bar{q}$ initial states in ref. [9].

(4), (5), and (6), can be defined and decomposed in an analogous fashion, with the colour and spin degrees of freedom of the final state gluon, quark q, or antiquark $\bar{q}$ being summed over.

In Born approximation $R^{(gg)}$ was given, e.g., in ref. [15]. In the computation of the order α_s^3 contributions we used dimensional regularization to treat both the ultraviolet and the infrared/collinear singularities. Renormalisation was performed using the $\overline{\mathrm{MS}}$ prescription for the QCD coupling α_s and the on-shell definition of the top mass m_t. The remaining soft and collinear singularities in $R^{(gg)}$, which appear as single and double poles in $\varepsilon = (4-D)/2$, are cancelled after including the contributions of $R^{(gg,g)}$ in the soft and collinear limits and after mass factorisation. For the latter we used the $\overline{\mathrm{MS}}$ factorisation scheme. The soft and collinear singularities of $R^{(gg,g)}$ were extracted by employing a simplified version of the phase-space slicing technique (cf. ref. [1] for details).

As a check of our calculation we computed the total cross section for $gg \to t\bar{t} + X$ at NLO. If one identifies the $\overline{\mathrm{MS}}$ renormalisation scale μ with the mass factorisation scale μ_F and neglects all quark masses except for m_t, then one can express the parton cross section in terms of dimensionless scaling functions [2]:

$$\hat{\sigma}_{gg}(\hat{s}, m_t^2) = \frac{\alpha_s^2}{m_t^2}[f_{gg}^{(0)}(\eta) + 4\pi\alpha_s(f_{gg}^{(1)}(\eta) + \tilde{f}_{gg}^{(1)}(\eta)\ln(\mu^2/m_t^2))], \tag{13}$$

where $\hat{s}$ is the parton c.m. energy squared and

$$\eta = \frac{\hat{s}}{4m_t^2} - 1. \tag{14}$$

Our results for these functions are shown in Fig. 1. The dotted line is the Born result $f_{gg}^{(0)}(\eta)$, the full line shows the function $f_{gg}^{(1)}(\eta)$, and the dashed line is $\tilde{f}_{gg}^{(1)}(\eta)$. We find excellent agreement with the corresponding results for $f_{gg}^{(0,1)}(\eta)$ of ref. [2, 4] and, after accounting for the different renormalisation schemes used by us and in ref. [2], with $\tilde{f}_{gg}^{(1)}(\eta)$.

The determination of $R^{(gq,q)}$ to order α_s^3, describing the (anti)quark-gluon subprocesses (5) and (6), involves initial state collinear singularities that we mass-factorised using the $\overline{\mathrm{MS}}$ factorisation scheme. The parton cross section $\hat{\sigma}_{gq}(\hat{s}, m_t^2)$ takes the form

$$\hat{\sigma}_{gq} = \frac{4\pi\alpha_s^3}{m_t^2}[f_{gq}^{(1)}(\eta) + \tilde{f}_{gq}^{(1)}(\eta)\ln(\mu^2/m_t^2))]. \tag{15}$$

The functions $f_{gq}^{(1)}(\eta)$ (full line) and $\tilde{f}_{gq}^{(1)}(\eta)$ (dashed line) are shown in Fig. 2. They agree perfectly with the corresponding results of ref. [2, 5]. The density matrix $R^{(g\bar{q},\bar{q})}$ can be obtained from $R^{(gq,q)}$ by exploiting the charge-conjugation invariance of QCD.

In order to exhibit the $t\bar{t}$ spin-correlation effects we consider now the following set of observables:

$$O_1 = 4\,\mathbf{s}_t \cdot \mathbf{s}_{\bar{t}}, \tag{16}$$

$$O_2 = 4\,(\hat{\mathbf{k}}_t \cdot \mathbf{s}_t)(\hat{\mathbf{k}}_{\bar{t}} \cdot \mathbf{s}_{\bar{t}}), \tag{17}$$

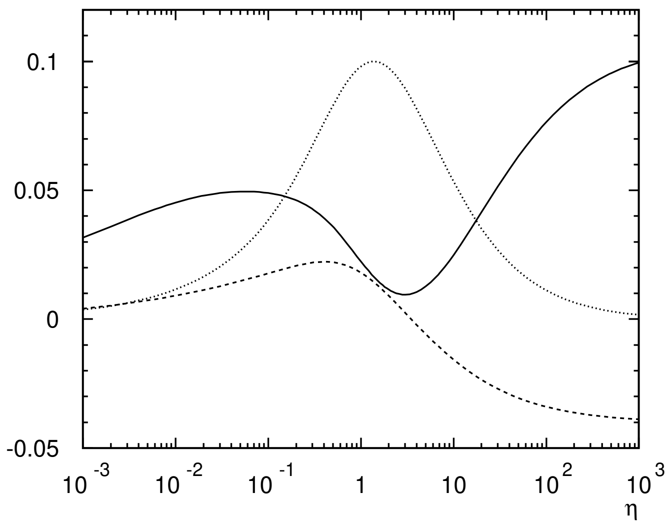

Figure 1: Dimensionless scaling functions $f_{gg}^{(0)}(\eta)$ (dotted), $f_{gg}^{(1)}(\eta)$ (full), and $\tilde{f}_{gg}^{(1)}(\eta)$ (dashed) that determine parton cross section $\hat{\sigma}_{gg}$.

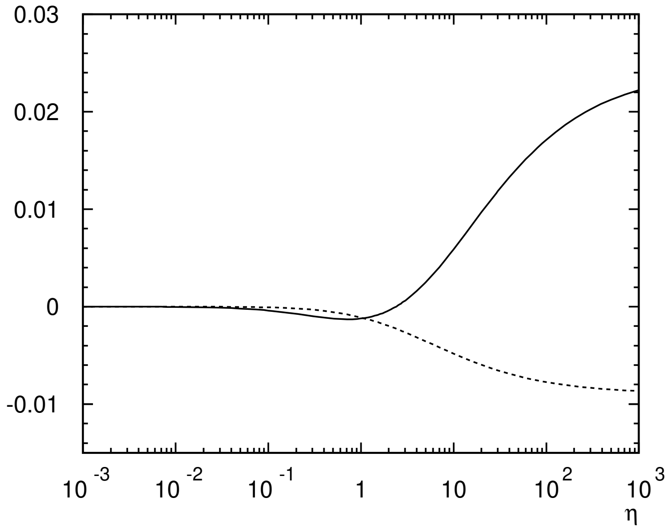

Figure 2: Dimensionless scaling functions $f_{gq}^{(1)}(\eta)$ (full) and $\tilde{f}_{gq}^{(1)}(\eta)$ (dashed) that determine $\hat{\sigma}_{gq}$.

$$O_3 = 4\,(\hat{\mathbf{p}}_1\cdot\mathbf{s}_t)(\hat{\mathbf{p}}_1\cdot\mathbf{s}_{\bar{t}}), \tag{18}$$

$$O_4 = 4\,(\hat{\mathbf{p}}_2^{*}\cdot\mathbf{s}_t)(\hat{\mathbf{p}}_1^{**}\cdot\mathbf{s}_{\bar{t}}), \tag{19}$$

where $\mathbf{s}_t = (\sigma\otimes 1\!\mathrm{l})/2$ and $\mathbf{s}_{\bar{t}} = (1\!\mathrm{l}\otimes\sigma)/2$ are the t and $\bar{t}$ spin operators and the factor 4 is conventional. The expectation values of the observables O_2, O_3 and O_4 determine the $t\bar{t}$ spin correlations using different spin quantisation axes. We consider here the fully inclusive case, i.e. integrate over the appropriate full final state phase space. Observable O_2 corresponds to a correlation of the t and $\bar{t}$ spins in the helicity basis, while O_3 correlates the spins projected along the beam line in the parton c.m.s. The 'beam-line basis' [16] used in O_4 refers to spin axes being parallel to $\hat{\mathbf{p}}_2^{*}$ and $\hat{\mathbf{p}}_1^{**}$, respectively. Here $\hat{\mathbf{p}}_2^{*}$ ($\hat{\mathbf{p}}_1^{**}$) is the direction of the downward (upward) collider beam in the t ($\bar{t}$) rest frame which we define by performing a rotation-free boost from the parton c. m. frame. The expectation values of O_2, O_3, and O_4 are related to the perhaps more familiar double spin asymmetries of the cross section as follows:

$$4\langle(\mathbf{a}\cdot\mathbf{s}_t)(\mathbf{b}\cdot\mathbf{s}_{\bar{t}})\rangle = \frac{\sigma(\uparrow\uparrow)+\sigma(\downarrow\downarrow)-\sigma(\uparrow\downarrow)-\sigma(\downarrow\uparrow)}{\sigma(\uparrow\uparrow)+\sigma(\downarrow\downarrow)+\sigma(\uparrow\downarrow)+\sigma(\downarrow\uparrow)}, \tag{20}$$

where the arrows refer to the spin state of the top quark (antiquark) using the unit vector **a** (**b**) as quantisation axis.

For the gg initial state we write the unnormalised expectation value of a spin-correlation observable O in analogy to eq. (13) as follows:

$$\hat{\sigma}_{gg}\langle O\rangle_{gg} = \frac{\alpha_s^2}{m_t^2}[g_{gg}^{(0)}(\eta)+4\pi\alpha_s(g_{gg}^{(1)}(\eta)+\tilde{g}_{gg}^{(1)}(\eta)\ln(\mu^2/m_t^2))]\,, \tag{21}$$

Our results for the functions $g_{gg}^{(0)}(\eta)$, $g_{gg}^{(1)}(\eta)$ and $\tilde{g}_{gg}^{(1)}(\eta)$ are shown for the four observables O_1–O_4 in Figs. 3–6. In each figure, the dotted line is the Born result $g_{gg}^{(0)}(\eta)$, the full line shows the function $g_{gg}^{(1)}(\eta)$, and the dashed line is $\tilde{g}_{gg}^{(1)}(\eta)$.

The QCD corrections to the unnormalised spin correlations are large close to threshold. This behaviour is due to the factor $\hat{\sigma}_{gg}$, which, in this order of perturbation theory, is non-zero at threshold due to Coulomb attraction. The corrections to the normalised partonic expectation values of all spin observables are tiny for small η. This is also the case for the contributions from $q\bar{q}$ annihilation [1]. For larger η, the spin correlations show a rich structure and the QCD corrections to the normalised expectation values can become significant. For hadronic observables, these effects are damped by the parton distribution functions and the QCD corrections are of the order of a few percent [17].

For the quark-gluon process (5) we represent the unnormalised expectation value of an observable in the form

$$\hat{\sigma}_{gq}\langle O\rangle_{gq} = \frac{4\pi\alpha_s^3}{m_t^2}[g_{gq}^{(1)}(\eta)+\tilde{g}_{gq}^{(1)}(\eta)\ln(\mu^2/m_t^2))]\,. \tag{22}$$

We have plotted in Figs. 7,8 the functions $g_{gq}^{(1)}(\eta)$, $\tilde{g}_{gq}^{(1)}(\eta)$ corresponding to the two observables O_2, O_3. The contributions of this channel to the spin correlations are very small.

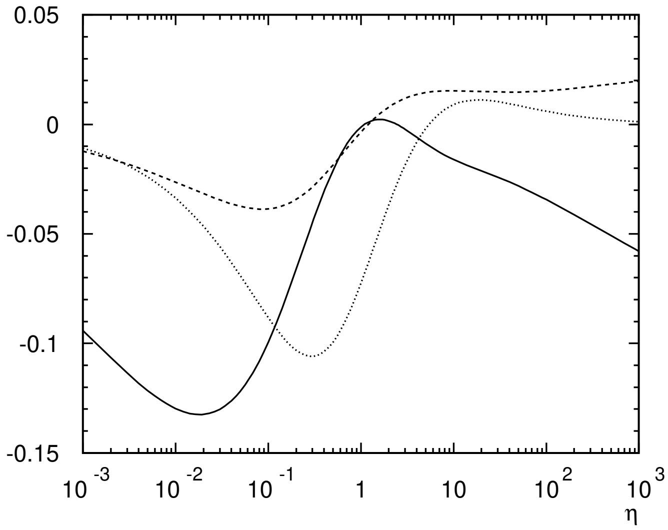

Figure 3: Dimensionless scaling functions $g_{gg}^{(0)}(\eta)$ (dotted), $g_{gg}^{(1)}(\eta)$ (full), and $\tilde{g}_{gg}^{(1)}(\eta)$ (dashed) that determine the expectation value $\hat{\sigma}_{gg}\langle \mathcal{O}_1 \rangle_{gg}$.

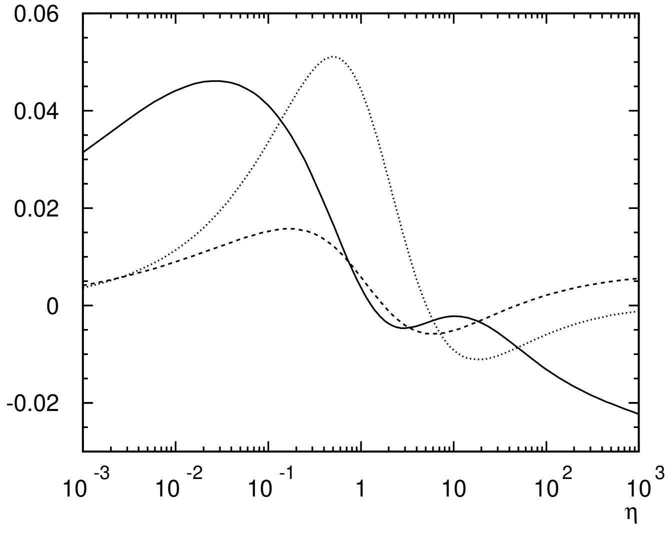

Figure 4: Same as Fig.1, but for $\hat{\sigma}_{gg}\langle \mathcal{O}_2 \rangle_{gg}$.

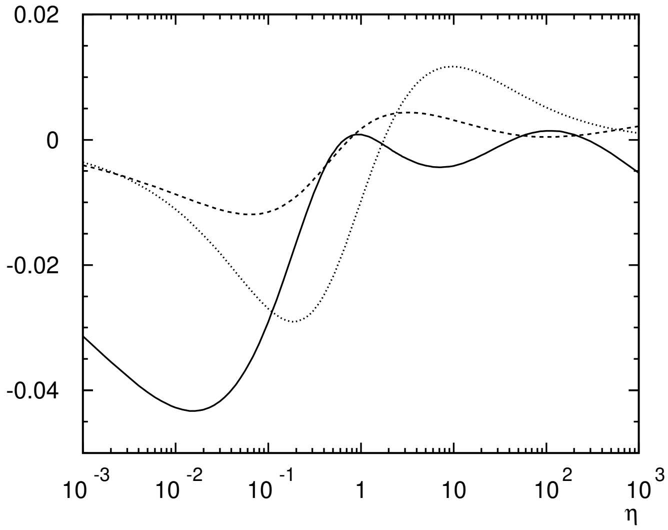

Figure 5: Same as Fig.1, but for $\hat{\sigma}_{gg}\langle O_3\rangle_{gg}$.

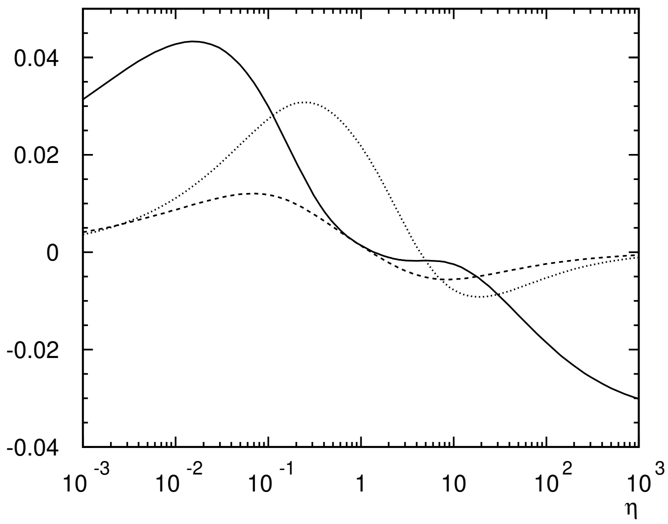

Figure 6: Same as Fig.1, but for $\hat{\sigma}_{gg}\langle O_4\rangle_{gg}$.

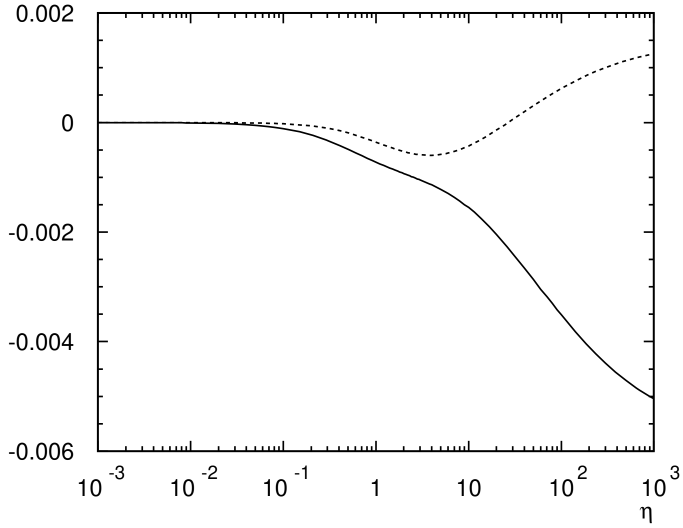

Figure 7: Dimensionless scaling functions $g_{gq}^{(1)}(\eta)$ (full) and $\tilde{g}_{gq}^{(1)}(\eta)$ (dashed) that determine the expectation value $\hat{\sigma}_{gq}\langle \mathcal{O}_2\rangle_{gq}$.

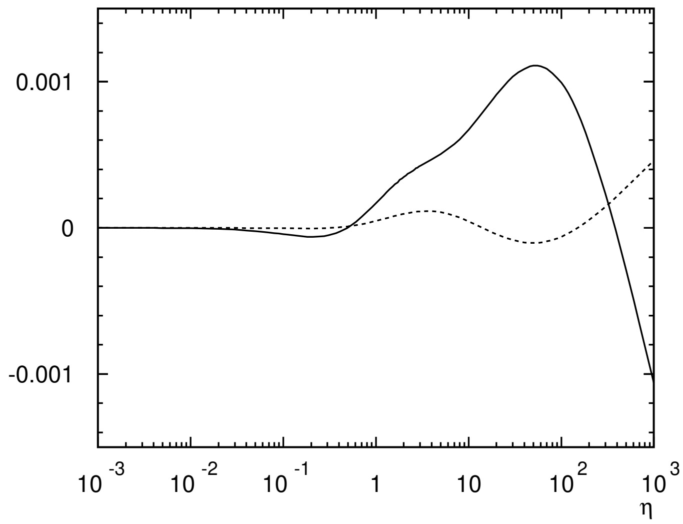

Figure 8: Same as Fig.7, but for $\hat{\sigma}_{gq}\langle \mathcal{O}_3\rangle_{gq}$.

In summary, we have computed the spin density matrices describing $t\bar{t}$ production by gluon-gluon and by (anti)quark-gluon fusion to order α_s^3. Together with our previous result on $R^{q\bar{q}}$ at NLO this work now provides the ingredients for a complete description of spin effects in the hadronic production of top quark pairs at NLO in the strong coupling, allowing for a more precise investigation of the $t\bar{t}$ production and decay processes.

References

[1] W. Bernreuther, A. Brandenburg and Z. G. Si, Phys. Lett. B483 (2000) 99 [hep-ph/0004184].

[2] P. Nason, S. Dawson and R. K. Ellis, Nucl. Phys. B 303 (1988) 607.

[3] P. Nason, S. Dawson and R. K. Ellis, Nucl. Phys. B 327 (1989) 49.

[4] W. Beenakker, H. Kuijf, W. L. van Neerven and J. Smith, Phys. Rev. D 40 (1989) 54.

[5] W. Beenakker, W. L. van Neerven, R. Meng, G. A. Schuler and J. Smith, Nucl. Phys. B 351 (1991) 507.

[6] M. Beneke *et al.*, hep-ph/0003033.

[7] R. G. Stuart, Phys. Lett. B 262 (1991) 113.

[8] A. Aeppli, G. J. van Oldenborgh and D. Wyler, Nucl. Phys. B 428 (1994) 126 [hep-ph/9312212].

[9] W. Beenakker, F. A. Berends and A. P. Chapovsky, Phys. Lett. B 454 (1999) 129 [hep-ph/9902304].

[10] A. Czarnecki, M. Jezabek and J. H. Kühn, Nucl. Phys. B 351 (1991) 70.

[11] C. R. Schmidt, Phys. Rev. D 54 (1996) 3250 [hep-ph/9504434].

[12] M. Fischer, S. Groote, J. G. Körner, M. C. Mauser and B. Lampe, Phys. Lett. B 451 (1999) 406 [hep-ph/9811482].

[13] W. Bernreuther, A. Brandenburg and P. Uwer, Phys. Lett. B 368 (1996) 153 [hep-ph/9510300].

[14] W. G. Dharmaratna and G. R. Goldstein, Phys. Rev. D 53 (1996) 1073.

[15] A. Brandenburg, Phys. Lett. B 388 (1996) 626 [hep-ph/9603333].

[16] G. Mahlon and S. Parke, Phys. Rev. D 53 (1996) 4886 [hep-ph/9512264] .

[17] W. Bernreuther, A. Brandenburg, Z. G. Si, and P. Uwer, work in progress.